Histol Histopathol (2017) 32: 805-816

**http://www.hh.um.es**

**Histology and Histopathology**

*From Cell Biology to Tissue Engineering*

# Ezrin and moesin expression in canine and feline osteosarcoma

**Juraj Hlavaty[1], Birgitt Wolfesberger[2], Marlene Hauck[3], Barbara Obermayer-Pietsch[4], Andrea Fuchs-Baumgartinger[5], Ingrid Miller[6] and Ingrid Walter[1,7]**

[1]Institute of Anatomy, Histology and Embryology, [2]Clinic for Companion Animal Medicine, Unit for Internal Medicine, University of Veterinary Medicine, Vienna, Austria, [3]Department of Clinical Sciences, College of Veterinary Medicine, North Carolina State University, Raleigh, North Carolina, USA, [4]Division of Endocrinology and Metabolism, Department of Internal Medicine, Medical University of Graz, Graz, [5]Institute of Pathology and Forensic Veterinary Medicine, [6]Institute of Medical Biochemistry and [7]VetCORE Facility for Research, University of Veterinary Medicine, Vienna, Austria

**Summary.** Biological features of canine osteosarcomas (OS) differ markedly from those found in feline and resemble more human osteosarcomas, in particular for their high rate of metastasis and poor prognosis. Ezrin, radixin and moesin are members of the ERM protein family and link the actin cytoskeleton with the cell membrane. Ezrin and moesin have been shown to be of prognostic significance in tumor progression due to their role in the metastatic process. The objective of this study was to analyze ezrin and moesin protein expression in a series of dog (n=16) and cat (n=8) osteosarcoma samples using immunohistochemistry and western blot techniques. We found that cat OS have a higher moesin expression compared to dog OS, however, the active phosphorylated forms of moesin and ezrin Tyr353 were more abundant in the dog samples. A statistically significant difference was found for the low and high immunohistochemical scores of ezrin and pan-phospho-ERM proteins between cat and dog. Although phospho-ezrin Thr567 was higher in feline OS, the membranous localization in dog OS samples indicates the presence of the biologically active form. Therefore, the observed differences in phosphorylated forms of ezrin and moesin status should be further studied to demonstrate if they are relevant for different biological behavior between dog and cat OS.

*Offprint requests to:* Ingrid Walter, Institute of Anatomy, Histology and Embryology, University of Veterinary Medicine, 1210 Vienna, Austria. e-mail: Ingrid.Walter@vetmeduni.ac.at

DOI: 10.14670/HH-11-848

**Key words:** Cat, Dog, Osteosarcoma, Ezrin, Moesin, Western blot

## Introduction

Osteosarcomas (OS) are the most frequent malignant bone tumors in dogs and cats (Priester and Mc Kay, 1980; Quigley and Leedale, 1983). Treatment options for this neoplasia include surgery, radiation therapy and chemotherapy. However, extended therapies are more usual for dogs than cats, the latter often demonstrating long term control after amputation alone, without any adjuvant treatment (Bitetto et al., 1987). It has been observed that only a minority of cats develop distant metastasis, whereas in contrast the majority of dogs die as a result of metastatic disease (Brodey and Riser, 1969; Dimopoulou et al., 2008). Similar to dogs the osteosarcoma of children and young adults is also highly aggressive and the prognosis is poor in patients with metastasis (Ta et al., 2009). Thus, identifying proteins which are primarily responsible for the development of metastases is particularly important for this disease.

Ezrin, a member of the ERM-(ezrin, radixin, moesin) family, which links the plasma membrane to the cytoskeleton, has been identified as a key component in tumor progression in several tumor types such as breast cancer, gastric cancer or osteosarcoma in humans (Khanna et al., 2004; Jin et al., 2012; Gschwantler-Kaulich et al., 2013). Experimental ezrin overexpression correlated with metastatic progression in human breast cancer cells, whereas ezrin silencing reversed this

behavior (Li et al., 2008). A significant association between expression pattern and prognosis has been reported, therefore, ezrin is a predictive marker for human osteosarcoma (Kim et al., 2007; Salas et al., 2007; Ferrari et al., 2008; Boldrini et al., 2010). Moreover, ezrin mRNA expression was significantly higher in human osteosarcomas with metastases compared to cases without metastases (Ogino et al., 2007).

OS are classified into several subtypes (osteoblastic, chondroblastic, teleangiectatic, fibroblastic, giant cell rich, multipatterned, poorly differentiated) according to the WHO classification system (Slayter et al., 1994). Ezrin expression has been related to the histological tumor subtype in human osteosarcoma: 30% of osteoblastic osteosarcomas did not express ezrin whereas all other investigated subtypes (fibroblastic, chondroblastic, telangiectatic) were almost generally positive (Ferrari et al., 2008). The relevance of tumor grading and the classification of OS subtypes have also been shown for the canine osteosarcoma (Loukopoulos and Robinson, 2017). To our best knowledge data about abundancy of ERM proteins and correlations with OS subtypes are not available for feline or canine osteosarcoma. A significant decrease of disease-free interval in the case of high ezrin expression has been reported (Khanna et al., 2004). The two functional stages of ezrin that can be discerned within normal and tumor cells are an inactive stage with the N- and C-terminal domains of the protein linked together forming a closed ring-like structure distributed within the cytoplasm, and an opened, active stage where it binds F-actin to the membrane via transmembrane proteins (Tsukita and Yonemura, 1997).

The localization of ezrin should be determined in tumor cells as it is associated with different functional stages of this protein. There was a significant reduction in disease-free survival time probability when ezrin was associated with the membrane in addition to being found in the cytoplasm (Krieg and Hunter, 1992). At least two events have been reported to induce the active ezrin stage - phosphorylation of a conserved threonine (Thr) residue at the aa position 567 and binding of a phosphatidyl inositol-4,5-bisphosphate molecule in so-called FERM domain of the protein (Matsui et al., 1998, 1999; Hamada et al., 2000). Ezrin and its phosphorylated form Thr567 have been demonstrated in human osteosarcoma; however, its permanent expression or overexpression per se was not sufficient for formation of primary tumors or lung metastases. Moreover, a dynamic regulation of ezrin phosphorylation has been suggested for tumor progression and metastasis formation (Ren et al., 2012). At least two other phosphorylation sites have been detected on the ezrin protein associated with its activation: Tyr353 and Tyr477 (Krieg and Hunter, 1992; Bretscher, 1999; Naba et al., 2008). In contrast to phospho-ezrin Thr567, which switches to the plasma membrane upon activation, ezrin phosphorylated at Tyr353 was found to be translocated into the nucleus in osteosarcomas (Di Cristofano et al., 2010). The expression of moesin, another member of the ERM family, has been correlated to cancer progression as well, but has been studied to a much lesser extent compared to ezrin. Increased moesin expression promotes epithelial-mesenchymal transition (EMT) in mammary epithelial cells by regulating adhesion and contractile elements for changes in actin filament organization (Haynes et al., 2011). High expression levels were detected in human metaplastic breast carcinomas as well as in non-mammary carcinosarcomas (Wang et al., 2012). Estecha and co-workers have shown that moesin is necessary for lung colonization by melanoma cells, a predominant site for osteosarcoma metastasis as well (Estecha et al., 2009). Even though the etiology of osteosarcoma is not fully known yet, dysregulation of multiple intracellular signaling pathways, especially the phosphatidylinositol 3-kinase (PI3K)/Akt pathway is important for OS onset and progression (for review see Zhang et al., 2014). A large body of evidence suggests that deregulation of this pathway has been involved in multiple pathological processes, including tumorigenesis, proliferation, invasion and metastasis - that means in processes where ERM-proteins involvement has been described as well (Levine et al., 2002; Krishnan et al., 2006; Zhang et al., 2014; Zhu et al., 2014).

There is a striking difference in the frequency of metastasis formation between canine and feline osteosarcoma, although the histopathological patterns are comparable (Dimopoulou et al., 2008). As it has been demonstrated by several investigators that ERM proteins could play an essential role in tumor progression, we hypothesized that there is a difference in ezrin and moesin expression and/or phosphorylation between the highly metastatic canine osteosarcoma and the low metastatic feline osteosarcoma. Moreover, the subcellular localization might vary in these species due to different behavior of the tumor cells. We tested this hypothesis by demonstrating the localization and distribution of ezrin and activated (phosphorylated) stages of ezrin, moesin, Akt and phosphorylated Akt in feline and canine osteosarcoma cells by means of immunohistochemistry and semi-quantitative protein analysis by western blotting.

## Material and methods

### *Tissue samples*

Clinical canine (n=16) and feline (n=8) OS samples were collected according to the rules of the ethical committee at the Veterinary University Vienna during therapeutical intervention (amputation or biopsy) or necropsy (animal data are summarized in Table 1). All investigated samples were primary osteosarcomas except one lung metastasis (dog 14) where we did not have access to the primary tumor. The information about the presence of metastases at time of diagnosis is summarized in Table 1. All samples were archived as

formaldehyde-fixed (4%) paraffin embedded (FFPE) specimens and fresh-frozen aliquots were stored at -170°C in the gas phase over liquid nitrogen in the VetBioBank of the Veterinary University Vienna. Samples were decalcified with 8% EDTA before embedding if necessary. Histologic diagnosis and subtypes of the OS were classified according to the criteria of the WHO (Slayter et al., 1994) and the histologic grade was determined using the grading system established by Kirpensteijn et al. (2002). This information is included in Table 1.

### *Cell lines*

Canine osteosarcoma D17 cells (ATCC No. CRL-6248) were routinely grown in Dulbecco's modified Eagle high glucose medium supplemented with 1% L-glutamine, 10% fetal calf serum, 1% antibiotic-antimycotic solution (all products purchased from Sigma-Aldrich, St. Louis MO, USA) in a tissue culture incubator at 37°C and 5% $CO_2$. For pellet preparation, cells were detached using trypsin (Sigma-Aldrich, Vienna, Austria) or scraped, washed with PBS and pelleted by centrifugation. For histological preparation, cell pellets were fixed in 4% formaldehyde for 24 h at 4°C, embedded in Histogel® (Richard-Allan Scientific, Microm International) as specified by the manufacturer, dehydrated and paraffin-embedded.

### *Immunohistochemistry*

Serial sections of each sample were cut at 3 $\mu$m and mounted on glutaraldehyde-APES-coated slides. After blocking unspecific staining by incubation in 1.5 % normal goat serum for 30 min at room temperature, sections were incubated with primary and secondary antibodies under conditions indicated in Table 2. Immunoreaction was developed with diaminobenzidine chromogen (D5905, Sigma-Aldrich). Nuclear counter-staining was done by hemalumn. Negative controls where the first antibody was substituted by PBS were included with every immunohistochemistry protocol. Positive controls were canine osteosarcoma cells (D17) and feline and canine kidney.

Immunostaining was evaluated by estimating the number of stained tumor cells (0%=0, ≤10%=1, ≤50%=2, ≥50%=3 of stained tumor cells) and the staining intensity (zero=0, mild=1, moderate=2, strong=3). Both values were multiplied to receive a total immunostaining score (IS) on one whole tumor section. Tumor center and invasive tumor front (tumor margin) were evaluated separately if available. Two-tailed Fisher's exact test was used calculate statistical significance of the immunoreactivity scores between dog

**Table 1.** Tumor samples: summary of animal data, tumor subtype and grade.

| Case no | Age | Sex | Breed | Tumor localization | Subtype | Grade | Amp/biop/necrop |
|---|---|---|---|---|---|---|---|
| dog | | | | | | | |
| 1 | 9y5mo | f/n | mixed | Humerus | osteoblastic | 2 | amp*[1] |
| 2 | 9y5mo | f/n | mixed | Humerus | osteoblastic | 2 | amp'[1] |
| 3 | 12y7mo | m | mixed | Anal sac | chondroblastic | 2 | biop |
| 4 | 7y | f | Leonberger | Tibia | osteoblastic | 2 | amp |
| 5 | 11y2mo | m/n | Dachshund | Scapula | osteoblastic | 2 | amp[1] |
| 6 | 8y | m/n | mixed | Humerus | fibroblastic | 3 | amp[1] |
| 7 | 5y3mo | f/n | Boxer | Radius | fibroblastic | 3 | amp |
| 8 | 8y3mo | f | St. Bernard | Radius | osteoblastic | 2 | amp[1] |
| 9 | 1y2mo | m | Rhodesian Ridgeback | Ulna | mixed | 2 | amp |
| 10 | 14y9mo | f | mixed | Mamma | osteoblastic | 2 | biop |
| 11 | 11y3mo | f | Munsterlander | Mandibula | osteoblastic | 3 | amp[1] |
| 12 | 7y3mo | m | mixed | Elbow | poorly diff. | 3 | amp |
| 13 | 9y | m/n | Dobermann | Femur | osteoblastic | 2 | amp |
| 14 | 7y1mo | f | Boxer | Lung/meta | telangiectatic | 3 | biop/metastasis |
| 15 | 12y6mo | f | mixed | Tibia | chondroblastic | 2 | necrop[1] |
| 16 | 8y7mo | f/n | Am. Staff. Terrier | Humerus | osteoblastic | 2 | amp |
| cat | | | | | | | |
| 17 | 11y11mo | m/n | Europ shorthair | Humerus | osteoblastic | 2 | amp[1] |
| 18 | 4y | m/n | Europ shorthair | Tibia | osteoblastic | 2 | necrop |
| 19 | 15y | m/n | Europ shorthair | Humerus | fibroblastic | 2 | amp |
| 20 | 8y | f/n | Europ shorthair | Skull | chondroblastic | na | biop |
| 21 | 13y | f/n | Europ shorthair | na | mixed | 1 | biop |
| 22 | 10y | f | Europ shorthair | Rib | fibroblastic | 1 | biop |
| 23 | na | na | Europ shorthair | Humerus | mixed | 2 | necrop |
| 24 | 6y | f/n | Europ. shorthair | na | osteoblastic | 1 | biop[1] |

F: female; m: male; n: neutered; *: soft part of tumor; ': hard part of tumor; na: not available; amp: amputation; biop: biopsy; necrop: necropsy; [1]: metastases at time of diagnosis of primary tumor confirmed.

and cat samples (for on-line calculator use http://www.socscistatistics.com/tests/fisher/Default2.aspx).

### *Western blotting protocol*

Protein lysates were prepared as described elsewhere (Scarlet et al., 2015). The protein concentration was estimated using DC™ Protein Assay (BioRad) according to the manufacterer's recommendations. The soluble, supernatant fraction was stored at -80°C until further analysis.

Protein extracts were separated on 10 % polyacrylamide gels for SDS-PAGE electrophoresis under reducing conditions and transferred to PVDF membrane (GE Healthcare, UK). Membranes were blocked using Western Blocking Reagent (Roche Diagnostics, Germany; dil. 1:10 in TBST) according to the manufacturer's recommendation to avoid unspecific antibody binding. Membranes were incubated with specific primary antibodies followed by secondary antibody incubation as indicated in Table 2. Proteins were visualized using Amersham Western Blotting Analysis System (GE Healthcare, UK). All antibodies were diluted in Western Blocking Reagent/TBST (1:10). Post immunodetection, films and membranes (post-stained with Coomassie R-250) were scanned with an Image Scanner III (GE Healthcare Life Sciences) and quantified by densitometry analysis using Quantity One software (version 4.4.0, Bio-Rad). Coomassie protein staining was used as a loading control and for normalization. A cell lysate from the well-known canine osteosarcoma cell line D-17 was analyzed as internal control in western blotting experiments.

## Results

### *Immunohistochemistry*

Immunohistochemical scores (IS) and cellular distribution are summarized in Table 3 and Table 4. Immunostaining for ezrin revealed moderate to strong cytoplasmic staining in all canine OS including a lung metastasis. In feline OS, ezrin distribution was also cytoplasmic, however, in contrast to canine OS not all feline tumors were positive for ezrin in the tumor cells and generally expressed a lower IS score. The canine OS cell line (D-17) showed a combination of both cytoplasmic and membrane staining with the anti-ezrin antibody (Figs. 1-8).

The phosphorylated form of pan-ERM proteins (ezrinThr567/radixinThr564/ moesinThr558) was predominantly located in the membrane in the D-17 canine osteosarcoma cell line. In the canine and feline OS tumor samples phospho-ezrin Thr567/radixinThr564/ moesinThr558 signal was also observed in the membranes, additionally, endothelia of blood vessels

**Table 2.** Sources, incubation conditions and dilutions of antibodies used in immunohistochemistry and Western blot analyses.

| Antibody | App. | Incubation time | Temp. | Dilution |
|---|---|---|---|---|
| Mouse monoclonal anti-ezrin (BD Transduction Laboratories, cat. # 610603) | IHC | ON | 4°C | 1:250 |
| | WB | ON | 4°C | 1:500 |
| Rabbit phospho-ezrin (Tyr353) (EnoGene, cat. # E011063, dil. 1:500) | IHC | ON | 4°C | 1:250 |
| | WB | ON | 4°C | 1:500 |
| Rabbit monoclonal phospho-ezrin (Thr567)/radixin (Thr564)/moesin (Thr558) (41A3) (Cell Signaling, cat. # 3149) | IHC | ON | 4°C | 1:250 |
| | WB | ON | 4°C | 1:500 |
| Rabbit monoclonal anti-moesin (Abcam, cat. # ab52490) | IHC | ON | 4°C | 1:250 |
| | WB | ON | 4°C | 1:500 |
| Rabbit polyclonal Akt (Cell Signaling, cat. # 9272) | WB | ON | 4°C | 1:1000 |
| Rabbit polyclonal phospho-Akt (Ser473) (Cell Signaling, cat. # 9271) | WB | ON | 4°C | 1:500 |
| Mouse monoclonal GAPDH (GeneTex, cat. # GTX627408) | WB | 10 min | RT | 1:3000 |
| Anti-mouse BrightVision Poly-HRP (ImmunoLogic, cat. # DPVM110HRP) | IHC | 30 min | RT | undil. |
| Anti-rabbit BrightVision Poly-HRP (ImmunoLogic, cat. # DPVR110HRP) | IHC | 30 min | RT | undil. |
| Amersham ECL-anti-mouse IgG peroxidase-linked species specific whole antibody from sheep (GE Healthcare, cat. # NA931) | WB | 30 min | RT | 1:5000 |
| Amersham ECL-anti-rabbit IgG peroxidase-linked species specific whole antibody from donkey (GE Healthcare, cat. # NA934) | WB | 30 min | RT | 1:5000 |

**Table 3.** Total immunohistochemical scores (IS) of canine and feline OS tumors.

| Score | Dog ezrin | Cat ezrin | Dog p-ezrinThr567 | Cat p-ezrinThr567 | Dog p-ezrinTyr353 | Cat p-ezrinTyr353 | Dog moesin | Cat moesin |
|---|---|---|---|---|---|---|---|---|
| - | 0 | 1 | 1 | 0 | 1 | 0 | 3 | 4 |
| + | 5 | 6 | 1 | 3 | 1 | 1 | 8 | 3 |
| ++ | 8 | 0 | 4 | 1 | 7 | 2 | 4 | 1 |
| +++ | 3 | 0 | 10 | 4 | 7 | 5 | 1 | 0 |

-: IS 0; +: IS 1 -3; ++: IS 4-6; +++: IS 7-9. cat ezrin 1 sample n.a.

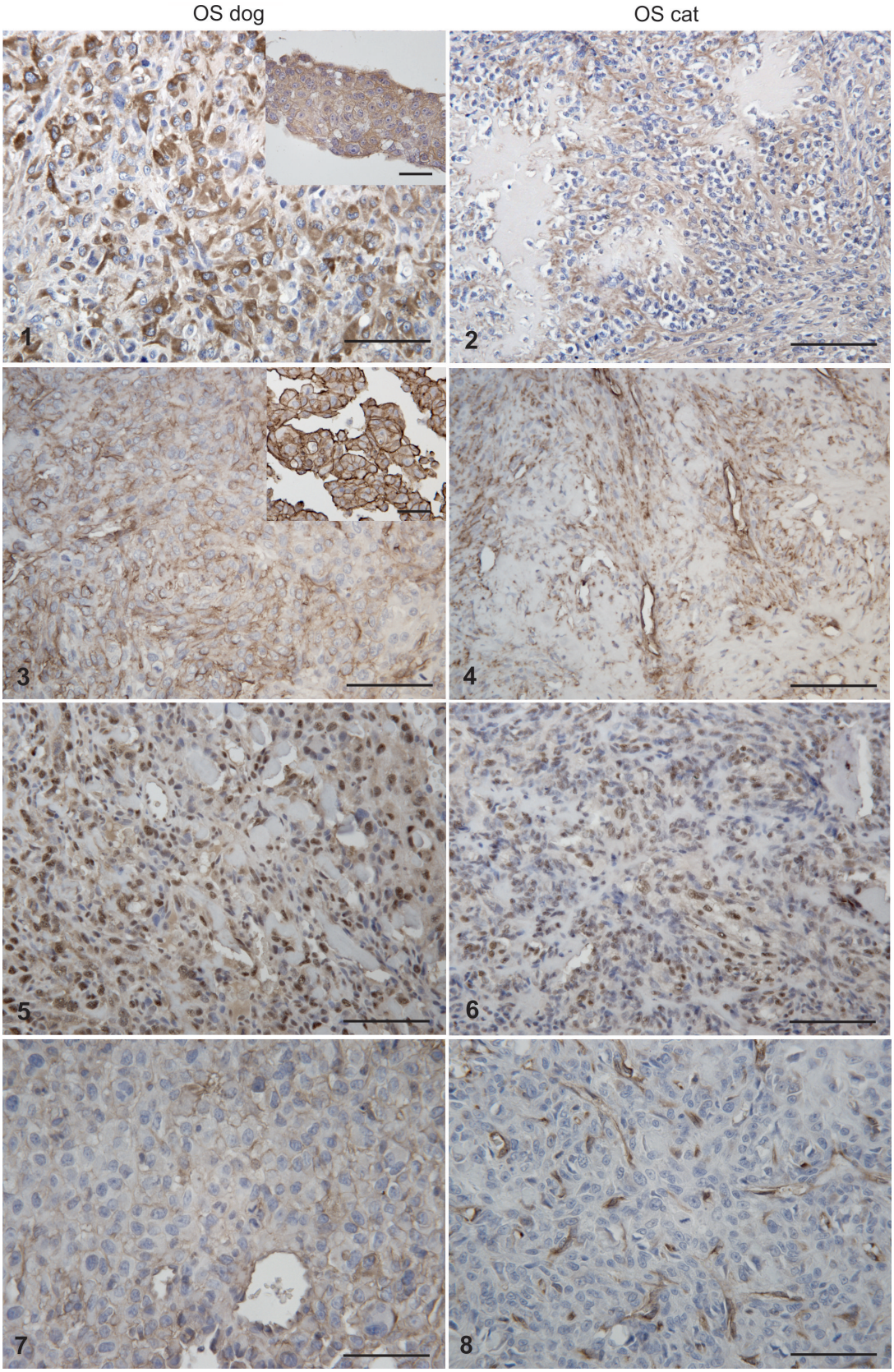


**Figs. 1-8.** Osteosarcoma; **Figure 1 and 2.** Erzin showed a cytoplasmic expression in canine (**1**, case No. 6) and feline (**2**, case No. 18) osteosarcoma. Insert shows D-17 canine OS cells. Immunohistochemistry. **Figure 3 and 4.** Phospho-ezrinThr567 was expressed in membranes and cytoplasm in canine (**3**, case No. 2) and feline (**4**, case No. 21) osteosarcoma sections. **Insert in figure 3** shows D-17 canine OS cells. Immunohistochemistry. **Figure 5 and 6.** Phospho-ezrin Tyr353 showed a predominant nuclear distribution in most samples of both species (**5**, case No. 1; **6**, case No. 22) after immunohistochemical staining. **Figure 7 and 8.** Examples of membranous moesin immunostaining in canine osteosarcoma (**7**, case No. 14) and staining of vascular endothelia in feline osteosarcoma (**8**, case No. 17) are shown. Scale bars: 100 $\mu$m, scale bars in inserts: 50 $\mu$m.

were strongly labelled. Strongest signal for phosphorylated pan-ERM proteins was present at the tumor margins in both species, whereas for non-phosphorylated ezrin almost no difference between tumor center and tumor margin was determined (Table 4). Most canine samples were found to be in the highest IS; only one canine sample was negative for pan phospho-ERM expression. All feline samples were positive (Figs. 3, 4) with a regular distribution within the IS (Table 3).

The phospho-ezrin form Tyr353 was localized in the nucleus in 13 of 16 canine OS samples, 6 had a cytoplasmic staining, one was negative. In cat 7 of 8 OS samples showed nuclear staining of phospho-ezrin Tyr353. An additional positive immunoreaction was observed in the cytoplasm of tumor cells in sections of both species (Figs. 5, 6). Phospho-ezrin Tyr353 immunostaining was stronger at the tumor margins in 40% of the feline OS samples but only in 15% of canine OS (Table 4).

Expression of moesin in tumor cells was moderate to weak in both species. Explicit membrane staining with anti-moesin was observed in some feline and canine OS including the lung metastasis. Moesin immunostaining clearly marked the endothelia of blood vessels in OS of both species in addition to the tumor cells (Figs. 7, 8). No differences between tumor front and tumor center were distinguishable for moesin expression (Table 4). Statistical evaluation of the low (IS score -/+) and high (IS score ++/+++) immunohistochemical score revealed significant differences ($p \leq 0.05$) in ezrin and pan-phospho-ERM reactivity between dog and cat samples, however the difference in p-ezrinTyr353 and moesin reactivity was not significant statistically. Concerning the primary samples with diagnosed metastasis at time of surgery and samples without confirmed metastasis there was no significant difference in the expression of ezrin or moesin or their phosphorylated forms as assessed by immunohistochemistry. The only lung metastasis that

**Table 4.** Immunohistochemical distribution of ezrin, phosphorylated ezrin and moesin in canine and feline osteosarcomas.

| Antibody | Nuclear positivity | | Cytoplasmatic positivity | | Membranous positivity | | Stronger staining on tumor front | |
|---|---|---|---|---|---|---|---|---|
| | cat | dog | cat | dog | cat | dog | cat | dog |
| ezrin | 0/8 (0%) | 0/16 (0%) | 7/8 (88%) | 16/16 (100%) | 0/0 (0%) | 0/0 (0%) | 0/5 (0%) | 1/13 (8%) |
| p-ezrin Thr567 | 0/8 (0%) | 0/16 (0%) | 4/8 (50%) | 4/16 (25%) | 4/8 (50%) | 15/16 (94%) | 2/5 (40%) | 8/13 (62%) |
| p-ezrin Tyr353 | 7/8 (88%) | 13/16 (81%) | 5/8 (63%) | 8/16 (50%) | 0/8 (0%) | 0/16 (0%) | 2/5 (40%) | 2/13 (15%) |
| moesin | 0/8 (0%) | 0/16 (0%) | 6/8 (75%) | 13/16 (81%) | 1/8 (13% ) | 3/16 (19%) | 0/5 (0%) | 0/13 (0%) |

Tumor front evaluation: only 5 cat samples and 13 dog samples were evaluated due to absence of tumor front on the other samples.

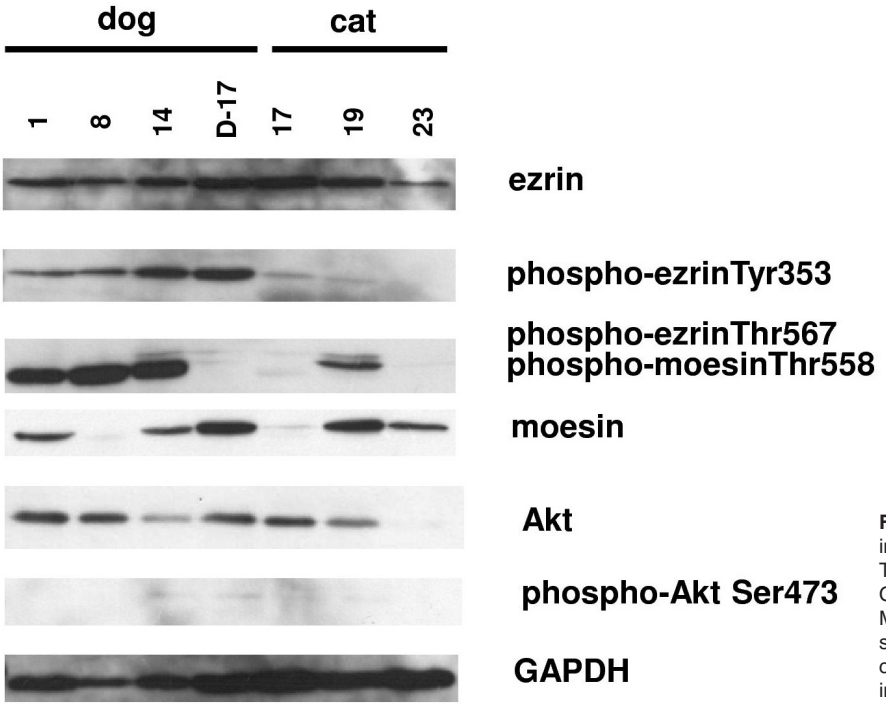


**Fig. 9.** Western blot detection of the ERM proteins in exemplary dog and cat osteosarcoma samples. Twenty micrograms of protein lysate from different OS subtypes were analyzed as described in Material and Methods section to confirm the specificity of the antibody. Cell lysate from canine osteosarcoma cell line D-17 was analyzed as internal control.

was evaluated showed highest immunohistochemical scores, except for pEzrin Tyr353 where it represented IS 6 (++). Positive controls for immunohistochemistry (feline and canine kidney) reacted as expected, negative controls were blank.

### *Western blot*

Western blot analysis of the osteosarcoma samples revealed similar ezrin expression in all samples of dog and cat OS (Tables 5, 6). However, a moesin band was only present in 82% of dog OS, while it was found in all cat OS in various expression levels. (Table 6, Figs. 9, 10).

Since ezrin phosphorylation status determines its activity in cellular processes, we next performed the analysis using a specific phospho-ezrin (Tyr353) antibody and a pan ERM phospho-ezrin (Thr567)/radixin (Thr564)/moesin (Thr558) antibody. The latter recognizes C-terminal specific threonine phosphorylation in all three forms of ERM proteins; however phosphorylated moesin at Thr558 differs in molecular weight slightly from phosphorylated forms of ezrin and radixin.

To clearly distinguish between signals specific for phospho-ezrin Thr567 and phospho-moesin Thr558, one exemplary cat OS and one dog OS sample were analyzed on a large scale slot, the membrane was cut into several strips and probed with respective antibodies (Fig. 11). The bands indicating ezrin, phospho-ezrin Tyr353 and phospho-ezrin Thr567 - upper band - migrated at the same molecular weight at about 80 kDa. The lower band detected with pan phospho-ezrin (Thr567)/radixin (Thr564)/moesin (Thr558) antibody at about 75-78 kDa correlated well with the band specific for moesin and therefore was considered as phospho-moesin Thr558.

Detailed analysis of canine and feline OS samples revealed higher expression of the phosphorylated form of moesin (Thr558) in dog samples as compared to cat OS (Fig. 9, Table 6). On the contrary, the latter samples showed higher expression of the phospho-ezrin Thr567 as compared to dog OS. Substantial differences in phospho-ezrin Tyr353 expression levels were observed between cat and dog OS (Table 6) with higher values in canine OS samples.

As the activation of ERM proteins can lead to the activation of the PI3K-Akt signaling pathway, we also examined Akt and phospho-Akt Ser473 status in these osteosarcoma samples (Fig. 9, Tables 5, 6). Whereas Akt signal was present in all samples with generally similar expression levels for both species, phospho-Akt Ser 473 signal was detected only in 3 out of 13 dog (23% positive) and 4 out of 7 cat (57% positive) OS at very low expression levels.

Western blot results are summarized in Table 5 and 6. No link between the tumor grade or subtype of OS (osteoblastic, fibroblastic, chondroblastic, teleangiectatic, mixed and poorly differentiated) and the amount of ezrin, moesin or the respective phosphorylated forms was found.

**Table 5.** Summary of western blot data.

| case no | ezrin | p-ezrin Tyr353 | p-ezrin Thr567 | moesin | p-moesin Thr558 | Akt | p-Akt Ser473 |
|---|---|---|---|---|---|---|---|
| dog | | | | | | | |
| 1 | +++ | ++ | - | ++ | ++++ | +++ | - |
| 2 | ++ | + | - | + | ++++ | + | - |
| 3 | +++ | +/++ | + | - | ++++ | ++ | + |
| 4 | + | -/+ | - | + | ++++ | nd | nd |
| 5 | +++ | +/++ | + | ++ | ++++ | +++ | + |
| 6 | ++ | + | + | + | ++++ | +++ | - |
| 7 | ++ | + | + | + | ++++ | nd | nd |
| 8 | +++ | ++ | - | + | ++++ | +++ | - |
| 9 | + | - | - | - | ++++ | ++ | - |
| 10 | +/++ | + | + | + | ++++ | -/+ | - |
| 11 | + | + | - | + | +++ | -/+ | - |
| 12 | ++ | ++/+++ | + | + | ++++ | ++ | - |
| 13 | + | + | + | + | ++++ | ++ | - |
| 14 | +++ | ++/+++ | + | ++ | ++++ | ++ | + |
| 15 | + | + | - | - | ++++ | ++ | - |
| 16 | ++ | +/++ | + | +/++ | ++++ | nd | nd |
| cat | | | | | | | |
| 17 | +++ | + | + | + | -/+ | +++ | + |
| 18 | ++ | + | +++ | + | +++ | ++ | + |
| 19 | ++ | + | ++ | +++ | +++ | ++/+++ | + |
| 20 | +/++ | - | ++ | -/+ | ++ | nd | nd |
| 21 | ++/+++ | + | ++ | ++ | +++ | ++ | + |
| 22 | ++/+++ | + | ++ | ++ | ++ | +++ | - |
| 23 | +/++ | -/+ | -/+ | ++ | ++ | + | - |
| 24 | ++ | -/+ | +/++ | + | + | +++ | - |

Na: not available; nd: not determined.

## Discussion

Osteosarcoma is the most common primary bone tumor in dog and cat as well, however dog OS behave differently compared with feline OS. Whereas high incidence of metastases (up to 90%) is described for dogs, only about 10% of feline OS are reported to metastasize (MacEwen, 1990; Dimopoulou et al., 2008). Considering aggressive local bone destruction and metastases occurrence, dog OS closely resembles the

**Table 6.** Western blot results of ezrin, moesin and Akt expression in dog and cat osteosarcomas.

| | Dog | Cat |
|---|---|---|
| ezrin | 16/16 (100%) | 8/8 (100%) |
| p-ezrin Thr567 | 11/16 (69%) | 8/8 (100%) |
| p-ezrin Tyr353 | 15/16 (94%) | 7/8 (88%) |
| moesin | 13/16 (82%) | 8/8 (100%) |
| p-moesinThr558 | 16/16 (100%) | 8/8 (100%) |
| Akt * | 13/13 (100%) | 7/7 (100%) |
| p-Akt Ser473 * | 3/13 (23%) | 4/7 (57%) |

*: 13 exemplary dog samples and 7 exemplary cat samples were analyzed.

human counterpart (Mueller et al., 2007; Fenger et al., 2014). Pulmonary parenchyma is the most common metastatic site for dog, cat and man (Quigley and Leedale, 1983; MacEwen 1990; Ferrari et al., 2008). The intention of our study was to determine and compare the presence of ERM proteins and their phosphorylation status in the highly aggressive canine OS and the low metastazing feline OS. Tumor metastasis is an important factor affecting survival time and mortality rate. Invasion and metastasis formation is a multistep process including invasion across the basal membrane by the tumor cells, intravasation into blood or lymph vessels, extravasation and growth at the new site (Sahai, 2007). During this process, cells undergo morphological changes driven by the cortical action of the cytoskeleton (Yamaguchi and Condeelis, 2007). Providing a regulated linkage between the plasma membrane and the actin cytoskeleton, the ERM family proteins are involved in determining cell shape, membrane and cell organization, division, migration, and signal transduction (Estecha et al., 2009; Arpin et al., 2011; Neisch and Fehorn, 2011). The metastatic process has been studied extensively in OS and several studies revealed a crucial role of the ERM protein family members in tumor dissemination (Curto and McClatchey, 2004; Fehon et al., 2010). Several processes of how ezrin might influence the metastatic process have been described, however the exact mechanism whereby ezrin contributes to metastasis formation is still not fully elucidated. High ezrin expression in dog and pediatric OS was associated with a significantly shorter median disease-free interval and with early development of metastases (Khanna et al., 2004). Using an osteosarcoma mouse model the same authors have also shown that ezrin is essential for tumor cell survival in the lung after migration from the tumor site and that early metastatic survival was partially dependent on activation of MAPK, but not AKT. However, unexpectedly, not constitutively phospho-

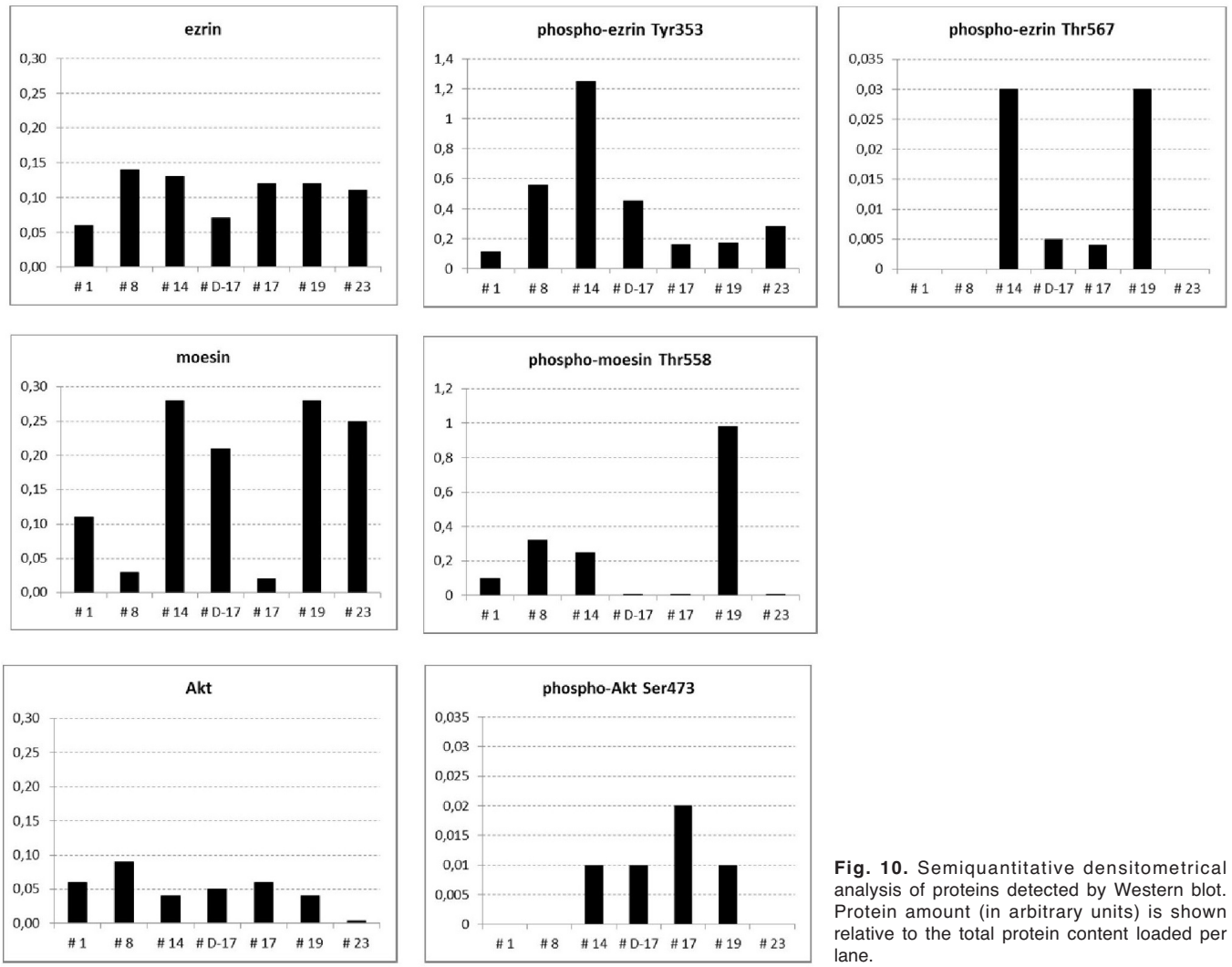


**Fig. 10.** Semiquantitative densitometrical analysis of proteins detected by Western blot. Protein amount (in arbitrary units) is shown relative to the total protein content loaded per lane.

rylated ezrin expression was sufficient for metastasis formation but only a dynamically regulated ezrin phosphorylation at Thr567 lead to metastatic progression in osteosarcoma (Bitteo et al., 1987). Furthermore, a critical role of ezrin for lung metastasis in OS was also demonstrated by Bulut et al. (2012). Two small molecules (NSC305787 and NSC668394) that inhibit ezrin significantly reduced lung metastases of OS cell lines in a mouse model via inhibition of phospho-ezrin Thr567 levels.

We have carefully analyzed the status of phospho-ezrin Thr567 in dog and cat samples using an immunohistochemical as well as a western blot approach. The rabbit monoclonal phospho-ezrin (Thr567)/radixin (Thr564)/moesin (Thr558) (41A3) antibody detects C-terminally phosphorylated forms of all three major ERM proteins and therefore the immunohistochemical analysis cannot distinguish between single phosphorylated proteins. On the contrary, western blot analysis using the antibody mentioned above provides a unique opportunity to discern between phosphorylated ezrin Thr567 and phosphorylated moesin Thr558 by comparing slight differences in the molecular weight of ezrin and moesin, as detected by their specific antibodies with signals obtained using the pan phospho-ERM antibody. Indeed, IHC analysis of all dog and cat samples using pan phospho-ERM antibody revealed positive staining in 15 out of 16 dog and 8 out of 8 cat osteosarcoma samples, respectively. However, there were major differences concerning the subcellular localization of the signal as determined by immunohistochemistry. Membranous staining, indicating the presence of active forms of ERM proteins, was seen in 94% of canine OS whereas only 50% of the feline OS expressed that pattern. Considering the cytoplasmic staining pattern we found 50% of the feline OS but only 25% of the canine OS positive. The numbers of cases in this study is too limited to perform a statistical analysis, so this must be investigated in further studies whether the higher metastatic potential in dog OS is due to the predominating membranous expression of ERM proteins. This would correlate with the findings of Ferrari et al. who reported a significantly longer free survival for patients with only cytoplasmic immunostaining compared to patients with membranous immunostaining in human OS (Ferrari et al., 2008).

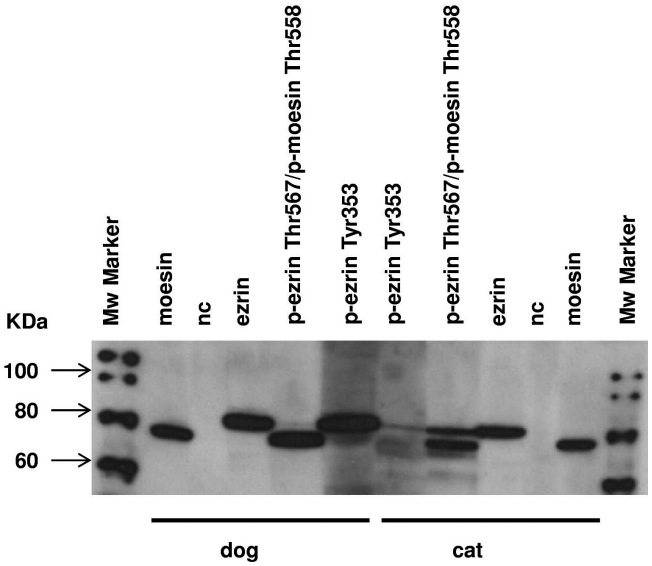


**Fig. 11.** Size differences between individual ERM proteins as observed in Western blot. The detected MW of ezrin, phospho-ezrin Tyr353 and phospho-ezrin Thr567 (MW ~ 80KDa) differ from the MW of moesin and phospho-moesin Thr558 proteins (MW <80KDa). Representative dog and cat samples are shown.

Minor discrepancies observed between immunohistochemical and western blot results could be due to the use of different sample parts of the heterogenous OS. Expression of ERM in blood vessels as has also been observed by immunohistochemistry in the present investigation might have an influence on western blotting results. It has been demonstrated that ERM proteins have important differential roles in the thrombin-induced modulation of endothelial cell permeability, with moesin promoting barrier dysfunction and radixin opposing it (Adyshev et al., 2013). It is well known that tumor blood vessels differ significantly from normal blood vessels concerning morphology and permeability (Hashizume et al., 2000), therefore, a closer look at the distribution and function of ERM proteins in tumor blood vessels will be needed.

Subsequent western blot analysis using pan phospho-ERM antibody discovered major differences between the levels of phospho-ezrin Thr567 and phospho-moesin Thr558 expression between dog and cat samples. It was obvious that phospho-moesin Thr558 was more abundant in the OS samples compared to phospho-ezrin Thr567 in both species. This contrast was especially distinct in the dog OS. While all samples were strongly positive for phospho-moesin Thr558, 5 out of 16 OS samples were negative for phospho-ezrin Thr567, whereas the remaining samples revealed only a weak signal corresponding to low amounts of phosphorylated protein. Interestingly, even though this trend was detected also in cat OS, levels of phospho-ezrin Thr567 were higher compared to dog OS and all tested samples were scored as positive. Using the pan ERM antibody in immunohistochemistry it is not possible to discern phospho-moesin Thr558, however, we interpreted the moesin membranous staining as the active/phosphorylated form.

The Akt kinase is known to activate ezrin by phosphorylation on Thr567, and osteosarcoma cells prone to pulmonary metastasis have elevated levels of phospho-Akt (Fukaya et al., 2005; Shiue et al., 2005). Although we have performed analysis of the Akt/p-Akt Ser473 status of the existing dog and cat osteosarcomas, due to low amount of positive samples (4 dogs and 4 cats) we cannot correlate these data to any osteosarcoma

subtype or to a specific pattern of the ERM protein expression.

Estecha and co-workers have shown that moesin is necessary for lung colonization by melanoma cells (Estecha et al., 2009). Moesin silencing markedly reduced the number of invasive cells and the depth of invasion. Interestingly, opposite roles for ezrin and moesin depletion were found in a 3D model of collagen invasion. Only moesin depletion impaired adhesion-dependent Rho kinase and subsequent myosin II activation in melanoma cells. As osteosarcoma cells also metastasize to the lung, moesin activation by phosphorylation is an important fact that should also be examined in feline and canine bone tumor. An emerging role of moesin and its phosphorylated form at Thr558 in glioma progression has been described recently (Zhu et al., 2013). Moesin was the major ERM member activated by phosphorylation in human glioblastoma cell lines. Binding to the CD44, a multistructural and multifunctional transmembrane receptor, moesin activated the PI3K-Akt, ERK, and p38MAPK pathways, induced β-catenin nuclear translocation and thereby specifically triggered the activation of β-catenin transcriptional activity. Interestingly, CD44 expression was also found in human osteosarcomas and in OS cell lines as well, and it was positively correlated with lung metastases (Benayahu et al., 2001; Gvozdenovic et al., 2013). Therefore, study of the interaction between moesin and CD44 molecule and its effect on the metastatic potential of dog and feline osteosarcomas remains an attractive topic to be elucidated. However, moesin phosphorylation on Thr558 is not the only known activation of the moesin molecule. G protein-coupled receptor kinases (GRK) phosphorylate moesin at the threonine Thr66 and regulate metastasis in prostate cancer (Chakraborty et al., 2014).

Much less data exist about the function and involvement of phospho-ezrin Tyr 353 in tumor or metastasis progression. In contrast to ezrin Thr567, which switches to the plasma membrane upon activation, ezrin phosphorylated at Tyr353 was found to be translocated into the nucleus in osteosarcomas (Di Cristofano et al., 2010). The exact mechanism of ezrin molecule translocation to the nucleus and its role there is not known yet, although its localization suggests a possible role as a nuclear factor in OS.

Summarizing, we found that cat OS have a higher moesin expression compared to dog OS, however, the active phosphorylated forms of moesin and ezrin Tyr353 were higher in the dog. Although ezrin Thr567 was higher in feline OS, the predominant membranous localization in dog OS samples as observed by immunohistochemistry indicates the presence of the biologically active form. Therefore, it could be speculated that the observed differences in phosphorylated forms of ezrin and moesin status in our pilot study between dog and cat OS could be one of the factors relevant for their different biological behavior. Further knowledge about biological differences of canine and feline OS could pave the way for novel therapeutic strategies for the treatment of this malignant disease.

*Acknowledgements.* The authors thank W. Tschulenk for expertise in western blotting, C. Höchsmann and A. Flemming for their excellent technical support in histology and immunohistochemistry. This research project was supported by the Austrian Science Fund (FWF) grant no. P23336-B11.

*Conflict of interest:* none.

## References

Adyshev D.M., Dudek S.M., Moldobaeva N., Kim K.M., Ma S.F., Kasa A., Garcia J.G. and Verin A.D. (2013). Ezrin/radixin/moesin proteins differentially regulate endothelial hyperpermeability after thrombin. Am. J. Physiol. Lung Cell. Mol. Physiol. 305, L240-L255.

Arpin M., Chirivino D., Naba A. and Zwaenepoel I. (2011). Emerging role for ERM proteins in cell adhesion and migration. Cell Adh. Migr. 5, 199-206.

Benayahu D., Shur I., Marom R., Meller I. and Issakov J. (2001). Cellular and molecular properties associated with osteosarcoma cells. J. Cell Biochem. 84, 108-114.

Bitetto W.V., Patnaik A.K., Schrader S.C. and Mooney S.C. (1987). Osteosarcoma in cats: 22 cases (1974-1984). J. Am. Vet. Med. Assoc. 190, 91-93.

Boldrini E., Peres S.V., Morini S. and de Camargo B. (2010). Immunoexpression of Ezrin and CD44 in patients with osteosarcoma. J. Pediatr. Hematol. Oncol. 32, e213-e217.

Bretscher A. (1999). Regulation of cortical structure by the ezrin-radixin-moesin protein family. Curr. Opin. Cell Biol. 11, 109-116.

Brodey R.S. and Riser W.H. (1969). Canine osteosarcoma. A clinicopathologic study of 194 cases. Clin. Orthop. Relat. Res. 62, 54-64.

Bulut G., Hong S.H., Chen K., Beauchamp E.M., Rahim S., Kosturko G.W., Glasgow E., Dakshanamurthy S., Lee H.S., Daar I., Toretsky J.A., Khanna C. and Uren A. (2012). Small molecule inhibitors of ezrin inhibit the invasive phenotype of osteosarcoma cells. Oncogene 31, 269-281.

Chakraborty P.K., Zhang Y., Coomes A.S, Kim W.J., Stupay R., Lynch L.D., Atkinson T., Kim J.I., Nie Z. and Daaka Y. (2014). G protein-coupled receptor kinase GRK5 phosphorylates moesin and regulates metastasis in prostate cancer. Cancer Res. 74, 3489-3500.

Curto M. and McClatchey A.I. (2004). Ezrin...a metastatic detERMinant? Cancer Cell 5, 113-114.

Di Cristofano C., Leopizzi M., Miraglia A., Sardella B., Moretti V., Ferrara A., Petrozza V. and Della Rocca, C. (2010). Phosphorylated ezrin is located in the nucleus of the osteosarcoma cell. Mod. Pathol. 23, 1012-1020.

Dimopoulou M., Kirpensteijn J., Moens H. and Kik M. (2008). Histologic prognosticators in feline osteosarcoma: a comparison with phenotypically similar canine osteosarcoma. Vet. Surg. 37, 466-471.

Estecha A., Sanchez-Martin L., Puig-Kröger A., Bartolomé R.A., Teixidó J., Samaniego R. and Sánchez-Mateos P. (2009). Moesin orchestrates cortical polarity of melanoma tumour cells to initiate 3D invasion. J. Cell Sci. 122, 3492-3501.

Fehon R.G., McClatchey A.I. and Bretscher A. (2010). Organizing the cell cortex: the role of ERM proteins. Nat. Rev. Mol. Cell Biol. 11,

276-287.
Fenger J.M., London C.A and Kisseberth W.C. (2014). Canine osteosarcoma: a naturally occurring disease to inform pediatric oncology. ILAR J. 55, 69-85.
Ferrari S., Zanella L., Alberghini M., Palmerini E., Staala E. and Bacchini P. (2008). Prognostic significance of immunohistochemical expression of ezrin in non-metastatic high-grade osteosarcoma. Pediat. Blood Cancer 50, 752-756.
Fukaya Y., Ishiguro N., Senga T., Ichigotani Y., Sohara Y., Tsutsui M., Shioura T., Iwamoto T. and Hamaguchi M. (2005). A role for PI3K-Akt signaling in pulmonary metastatic nodule formation of the osteosarcoma cell line, LM8. Oncol. Rep. 14, 847-852.
Gschwantler-Kaulich D., Natter C., Steurer S., Walter I., Thomas A., Salama M. and Singer C.F. (2013). Increase in ezrin expression from benign to malignant breast tumours. Cellular Oncol. (Dordr.) 36, 485-491.
Gvozdenovic A., Arlt M.J.E., Campanile C., Brennecke P., Husmann K., Li Y., Born W., Muff R. and Fuchs B. (2013). CD44 enhances tumor formation and lung metastasis in experimental osteosarcoma and is an additional predictor for poor patient outcome. J. Bone Miner. Res. 28, 838-847.
Hamada K., Shimizu T., Matsui T., Tsukita S. and Hakoshima T. (2000). Structural basis of the membrane-targeting and unmasking mechanisms of the radixin FERM domain. EMBO J. 19, 4449-4462.
Hashizume H., Baluk P., Morikawa S., McLean J.W., Thurston G., Roberge S., Jain R.K. and McDonald D.M. (2000). Openings between defective endothelial cells explain tumor vessel leakiness. Am. J. Pathol. 156, 1363-1380.
Haynes J., Srivastava J., Madson N., Wittmann T. and Barber D.L. (2011). Dynamic actin remodeling during epithelial-mesenchymal transition depends on increased moesin expression. Mol. Biol. Cell 22, 4750-4764.
Jin J., Jin T., Quan M., Piao Y. and Lin Z. (2012). Ezrin overexpression predicts the poor prognosis of gastric adenocarcinoma. Diagn. Pathol. 7, 135-143.
Khanna C., Wan X., Bose S., Cassaday R., Olomu O., Mendoza A., Yeung C., Gorlick R., Hewitt S.M. and Helman L.J. (2004). The membrane-cytoskeleton linker ezrin is necessary for osteosarcoma metastasis. Nat. Med. 10, 182-186.
Kim M.S., Song W.S., Cho W.H., Lee S.Y. and Jeon D.G. (2007). Ezrin expression predicts survival in stage IIB osteosarcomas. Clin. Orthop. Relat. Res. 459, 229-236.
Kirpensteijn J., Kik M., Rutteman G.R. and Teske E. (2002). Prognostic significance of a new histologic grading system for canine osteosarcoma. Vet. Pathol. 39, 240-246.
Krieg J. and Hunter T. (1992). Identification of the two major epidermal growth factor-induced tyrosine phosphorylation sites in the microvillar core protein ezrin. J. Biol. Chem. 267, 19258-19265.
Krishnan K., Bruce B., Hewitt S., Thomas D., Khanna C. and Helman L.J. (2006). Ezrin mediates growth and survival in Ewing's sarcoma through the AKT/mTOR, but not the MAPK, signaling pathway. Clin. Exp. Metastasis 23, 227-236.
Levine R.A., Forest T. and Smith C. (2002). Tumor suppressor PTEN is mutated in canine osteosarcoma cell lines and tumors. Vet. Pathol. 39, 372-378.
Li Q., Wu M., Wang H., Xu G., Zhu T., Zhang Y., Liu P., Song A., Gang C., Han Z., Zhou J., Meng L., Lu Y., Wang S. and Ma D. (2008). Ezrin silencing by small hairpin RNA reverses metastatic behaviors of human breast cancer cells. Cancer Lett. 261, 55-63.
Loukopoulos P. and Robinson W.F. (2007). Clinicopathological relevance of tumour grading in canine osteosarcoma. J. Comp. Pathol. 136, 65-73.
MacEwen E.G. (1990). Spontaneous tumors in dogs and cat: models for the study of cancer biology and treatment. Cancer Met. Rev. 9, 125-136.
Matsui T., Maeda M., Doi Y., Yonemura S., Amano M., Kaibuchi K., Tsukita S. and Tsukita S. (1998). Rho-kinase phosphorylates COOH-terminal threonines of ezrin/radixin/moesin (ERM) proteins and regulates their head-to-tail association. J. Cell Biol. 140, 647-657.
Matsui T., Yonemura S., Tsukita S. and Tsukita S. (1999). Activation of ERM proteins in vivo by Rho involves phosphatidyl-inositol 4-phosphate 5-kinase and not ROCK kinases. Curr. Biol. 9, 1259-1262.
Mueller F., Fuchs B. and Kaser-Hotz B. (2007). Comparative biology of human and canine osteosarcoma. Anticancer Res. 27, 155-164.
Naba A., Reverdy C., Louvard D. and Arpin M. (2008). Spatial recruitment and activation of the Fes kinase by ezrin promotes HGF-induced cell scattering. EMBO J. 27, 38-50.
Neisch A.L. and Fehon R.G. (2011). Ezrin, radixin and moesin: key regulators of membrane-cortex interactions and signaling. Curr. Opin. Cell Biol. 23, 373-382.
Ogino W., Takeshima Y., Mori T., Yanai T., Hayakawa A., Akisue T., Kurosaka M. and Matsuo M. (2007). High level of ezrin mRNA expression in an osteosarcoma biopsy sample with lung metastasis. J. Pediat. Hematol. Oncol. 29, 435-439.
Priester W.A. and Mc Kay F.W. (1980). The occurrence of tumors in domestic animals. J. Natl. Cancer Inst. Monogr. 54, 1-210.
Quigley P.J. and Leedale A.H. (1983). Tumors involving bone in the domestic cat: A review of fifty-eight cases. Vet. Pathol. 20, 670-686.
Ren L., Hong S.H., Chen Q.R., Briggs J., Cassavaugh J., Srinivasan S., Lizardo M.M., Mendoza A., Xia A.Y., Avadhani N., Khan J. and Khanna C. (2012). Dysregulation of ezrin phosphorylation prevents metastasis and alters cellular metabolism in osteosarcoma. Cancer Res. 72, 1001-1012.
Sahai E. (2007). Illuminating the metastatic process. Nat. Rev. Cancer 7, 737-749.
Salas S., Bartoli C., Deville J.L., Gaudart J., Fina F., Calisti A., Bollini G., Curvale G., Gentet J.C., Duffaud F., Figarella-Branger D. and Bouvier C. (2007). Ezrin and alpha-smooth muscle actin are immunohistochemical prognostic markers in conventional osteosarcomas. Virchows Arch. 451, 999-1007.
Scarlet D., Walter I., Hlavaty J. and Aurich C. (2015). Expression and immunolocalisation of follicle-stimulating hormone receptors in gonads of newborn and adult female horses. Reprod. Fertil. Dev. (in press).
Shiue H., Musch M.W., Wang Y., Chang E.B. and Turner, J.R. (2005). Akt2 phosphorylates ezrin to trigger NHE3 translocation and activation. J. Biol. Chem. 280, 1688-1695.
Slayter M.V., Boosinger T.R., Pool R.R., Dämmrich K., Misdorp W. and Larsen S. (1994). Histological Classification of Bone and Joint Tumors of Domestic Animals. 2nd series, Vol I, Published by the Armed Forces Inst. of Pathology in cooperation with the American Registry of Pathology and the World Health Organization (WHO), Washington D.C.
Ta H.T., Dass C.R., Choong P.F. and Dunstan D.E. (2009). Osteosarcoma treatment: state of the art. Cancer Metastasis Rev. 28, 247-263.

Tsukita S. and Yonemura S. (1997). ERM proteins: head-to-tail regulation of actin-plasma membrane interaction. Trends Biochemical Sci. 22, 53-58.

Wang C.C., Liau J.Y., Lu Y.S., Chen J.W., Yao Y.T. and Lien H.C. (2012). Differential expression of moesin in breast cancers and its implication in epithelial-mesenchymal transition. Histopathology 61, 78-87.

Yamaguchi H. and Condeelis J. (2007). Regulation of the actin cytoskeleton in cancer cell migration and invasion. Biochim. Biophys. Acta 1773, 642-652.

Zhang A., He S., Sun X., Ding L., Bao X. and Wang N. (2014). Wnt5a promotes migration of human osteosarcoma cells by triggering a phosphatidylinositol-3 kinase/Akt signals. Cancer Cell. Int. 14, 15.

Zhu X., Morales F., Agarwal N.K., Dogruluk T., Gagea M. and Georgescu M.M. (2013). Moesin is a glioma progression marker that induces proliferation and Wnt/β-catenin pathway activation via interaction with CD44. Cancer Res. 73, 1142-1155.

Zhu L.B., Jiang J., Zhu X.P., Wang T.F., Chen X.Y., Luo Q.F., Shu Y., Liu Z.L. and Huang S.H. (2014). Knockdown of Aurora-B inhibits osteosarcoma cell invasion and migration via modulating PI3K/Akt/NF-κB signaling pathway. Int. J. Clin. Exp. Pathol. 7, 3984-3991.

Accepted November 30, 2016